Surface structure and long-range order of the Ge(111)-$c(2\times8)$ reconstruction

R. Feidenhans'l, J. S. Pedersen, J. Bohr, and M. Nielsen
Risø National Laboratory, P.O. Box 49, DK-4000 Roskilde, Denmark

F. Grey* and R. L. Johnson
Max-Planck-Institut for Solid State Research, P.O. Box 80 06 65, D-7000 Stuttgart 80, Federal Republic of Germany
(Received 24 March 1988)

We have performed an x-ray diffraction study of the Ge(111)-$c(2\times8)$ surface. From the analysis of 43 in-plane, symmetry-inequivalent structure factors, a simple adatom model with subsurface relaxation is deduced. The relaxations around the adatoms are similar to those observed in the adatom complexes on Si(111)-(7×7) and Sn/Ge(111)-$(\sqrt{3}\times\sqrt{3})$, -(5×5), and -(7×7), suggesting that the adatoms are located in threefold sites above the second-layer atoms (T_4 sites). Significant distortions around the rest atoms are seen due to rehybridization of the dangling bonds. The diffraction peaks from the eighth-order reflections are displaced away from their nominal positions. This is explained by a model where the long-range order of the $c(2\times8)$ structure is disturbed by faults due to rows of 2×2 unit cells.

I. INTRODUCTION

Normally the equilibrium reconstruction of the (111) surfaces of group-IV elemental semiconductors is either 5×5 [$Ge_xSi_{1-x}Si(111)$ (Refs. 1–3) or Sn/Ge(111) (Ref. 4)] or 7×7 [Si(111),[5] $Ge_xSi_{1-x}Si(111)$,[1–3] Sn/Ge(111),[4] or Ge(111) under lateral compressive strain[6]]. All these surfaces can be described in terms of the dimer-adatom-stacking fault (DAS) model derived by Takayanagi *et al.* for Si(111)-(7×7).[7,8] This has initiated a great interest in the universal behavior of the (111) surfaces in order to reveal the driving mechanism behind the 5×5 or 7×7 reconstructions.[8,9] There is one exception from the general picture, namely the clean, unstrained Ge(111) surface which has a $c(2\times8)$ structure.[10–12] Any unified description of the (111) surfaces must be able to include the Ge(111)-$c(2\times8)$ surface and explain its deviation from the DAS model. It is therefore of great importance to determine the atomic geometry of this structure.

Scanning tunneling microscopy (STM) images have shown that the structure has adatoms which are arranged such that each $c(2\times8)$ unit cell consists of one 2×2 and one $c(4\times2)$ subunit.[13,14] Recently two models incorporating this adatom pattern have been proposed. Using adatom clusters as building blocks for the DAS model, Takayanagi *et al.* constructed a model which explains both 5×5, 7×7, and $c(2\times8)$ reconstructions.[8] The adatom cluster consisted of one adatom bonded to three underlying atoms and could be placed in regions with either regular or reversed stacking. The walls between the two types of stacking were chains of dimers. The model is called the dimer-chain model[8] and has the same adatom arrangement as that observed with STM.[4]

Based on total-energy considerations, Vanderbilt could explain the overall behavior of the (111) surfaces of Si and Ge with the assumption that the $c(2\times8)$ structure only consists of the decoration with adatoms as seen with STM (Ref. 14) with no major rearrangement of the substrate atoms.[9] This simple adatom model has also been proposed by Mareé *et al.* using medium-energy ion scattering[15] and is shown in Fig. 1(a). Their experimental data is controversial since it shows considerably less distortion for the Ge(111)-$c(2\times8)$ surface than for Si(111)-(7×7) which disagrees with previous ion-scattering stud-

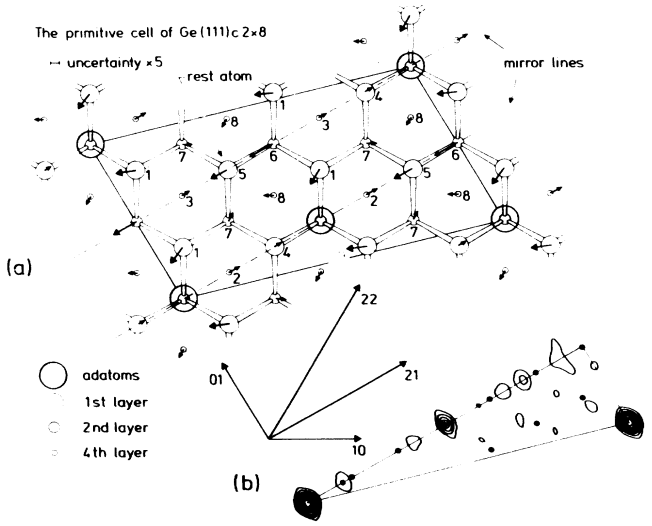

FIG. 1. (a) The primitive cell of the $c(2\times8)$ structure with adatoms in T_4 sites and subsurface relaxations. The independent atoms in the analysis are labeled 1–8. The third-layer substrate atoms are situated directly below the second-layer atoms and therefore not shown. The displacements derived from the least-squares analysis are multiplied by five and shown as arrows. The triangle enclosed by a mirror line and the cell edges is the irreducible unit for the Patterson function shown in (b). The estimated uncertainty, multiplied by five, is indicated. It applied radially and transverse to the displacements for all atoms, except those on the mirror lines where it only applied radially. The scale is given by the length of the (1,0) vector which is $a_0/\sqrt{2}=4.0$ Å. (b) The contour plot of the Patterson function. Only positive levels are shown. Projections of bulk interatomic vectors onto the surface plane are shown as solid circles. The scale is the same as in (a).

ies.[16] We present here a surface x-ray diffraction study which demonstrates the validity of the simple adatom model provided subsurface relaxations over at least three atomic layers are included. Furthermore, we show that the long-range order of the $c(2\times8)$ adatom pattern is destroyed by faults in the form of rows of 2×2 unit cells.

II. EXPERIMENTAL

The Ge(111) surface was cleaned by 500-eV Ar^+-ion bombardement and subsequent annealing to 750 °C. This procedure was repeated until the low-energy electron diffraction (LEED) pattern had sharp $c(2\times8)$ diffraction spots and angle-integrated photoemission spectra showed no traces of impurities. The sample was then transferred to a small portable UHV cell for x-ray diffraction, which was mounted on the vertical scattering diffractometer at the 32-pole wiggler-beamline W1 at Hamburg Synchrotron Radiation Laboratory (HASYLAB). Two flat Ge(111) crystals in conjunction with a toroidal Au-plated mirror were used to monochromatize the x-ray beam to a wavelength of 1.345 Å. The diffractometer was aligned so that the x-ray beam has a fixed glancing angle to the sample surface of 0.274°, which is the critical angle for total external reflection. This gives a penetration depth of intensity into the surface of 190 Å. A 1-mm slit placed just before the sample and a 2-mm slit mounted on the detector arm just after the sample defined the active area of the surface. The in-plane acceptance of the detector was 0.7°. A total of 64 integrated intensities from in-plane fractional-order reflections were measured of which 43 were non-symmetry-equivalent half- and eighth-order reflections and four quarter-order reflections.

III. DATA ANALYSIS

Due to the low symmetry of the $c(2\times8)$ unit cell, three 120° rotational-equivalent domains exist on the surface with no overlap of fractional-order reflections. The intensity ratio of symmetry-equivalent reflections from each domain was 1.3:1.0:0.7, presumably due to a slight miscut of the surface which induces a preferred orientation of the domains. The integrated intensities were adjusted for this effect and corrected for Lorentz factor $\{[\sin(2\theta)]^{-1}\}$ and variations in active sample area $\{[\sin(2\theta)]^{-1}\}$ in order to give the structure factor intensities shown in Fig. 2. There is some uncertainty in the intensities due to disorder in the $c(2\times8)$ structure illustrated in Fig. 3. All eighth-order reflections are broadened and displayed away from their nominal positions and there is a tail of scattering between the half- and eighth-order reflections. The overlap between the reflections means that true integrated intensities cannot be recorded and the errors may be larger than the uncertainties from counting statistics and reproducibility between symmetry-equivalent reflections. We will therefore give all structure factors equal weight in the structural analysis by using an R ("reliability") factor given by

$$R=\left[\frac{\sum(|F_o|-|F_c|)^2}{\sum|F_o|^2}\right]^{1/2} \quad (1)$$

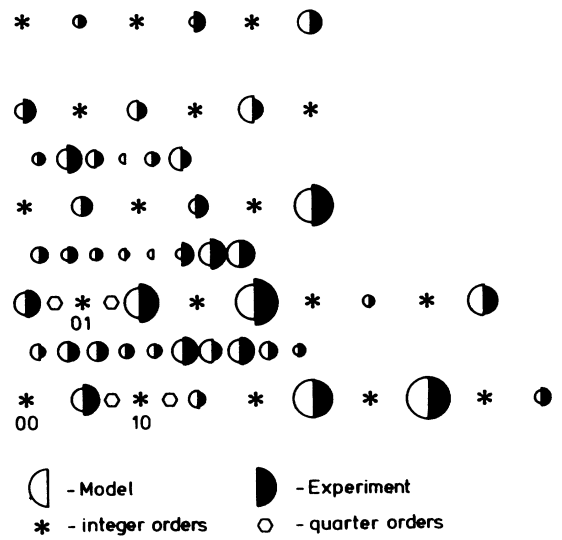

FIG. 2. The structure factor pattern of a single $c(2\times8)$ domain, showing the agreement between the experimental data and the model in Fig. 1(a). The radii of the half-circles are proportional to the structure factor amplitudes, the area to the intensities. The four measured quarter-order reflections are indicated by hexagons.

to quantify the agreement between model and experiment. F_o and F_c are the observed and calculated structure factors, respectively.

The intensities of the four quarter-order reflections measured were all zero within uncertainties estimated to ~2% of the intensity of the largest half-order reflections.

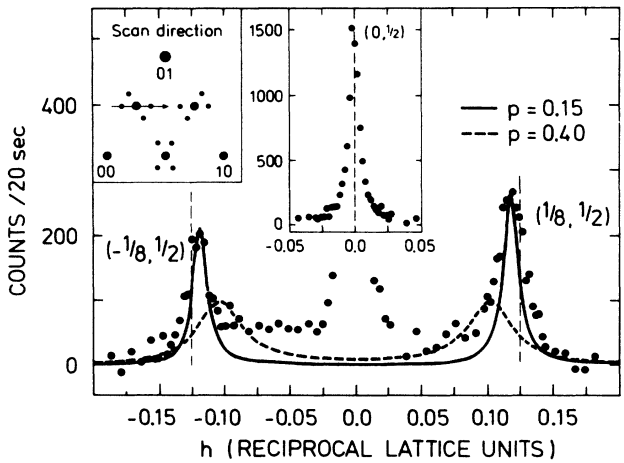

FIG. 3. A scan in the (10) direction through the $(-\frac{1}{8}\frac{1}{2})$, $(0\frac{1}{2})$ and $(\frac{1}{8}\frac{1}{2})$ reflections, showing the displacements of the eighth-order peaks. The width of the $(0\frac{1}{2})$ peak is given by a domain size of ~600 Å. The solid curve shows the intensity distribution given by Eq. (5) with 2×2 unit cells with a probability $p=0.15$. The curve is scaled such that it has the same peak heights as the experimental data. The dashed curve has $p=0.40$. The $(0\frac{1}{2})$ reflection belongs to a different domain than the $(-\frac{1}{8}\frac{1}{2})$ and $(\frac{1}{8}\frac{1}{2})$ reflections and is therefore not included in the theoretical curves.

This is in agreement with recent LEED observations where it was possible to detect very weak quarter-order reflections.[17] We therefore conclude that within our experimental accuracy all quarter-order reflections are missing. This means that the atoms in the $c(2\times8)$ unit cell can be grouped in pairs.[11,12] The two atoms in a pair are interconnected by a (2,1) or (2,2) vector (see Fig. 1), which assures a vanishing structure factor for quarter-order reflections from each pair. This is not in agreement with the dimer-chain model.[18] In fact, we have to exclude the dimer-chain model on the basis of the four missing quarter-order reflections *alone*.

A contour plot of the Patterson or pair correlation function, the Fourier inversion of the structure-factor intensities, is shown in Fig. 1(b). This gives a map of interatomic vectors occurring within the $c(2\times8)$ unit cell.[18] The plot shows one clear nonorigin vector, namely (2,1). The simplest possible model with this interatomic vector is the simple adatom model (without subsurface relaxation) as shown in Fig. 1(a). The structure factors for this model, apart from atomic form and Debye-Waller factors, are

$$F_{hk}=\begin{cases}2 & \text{for half-order reflections}\\ 1\pm i & \text{for eighth-order reflections}\end{cases}. \tag{2}$$

Clearly, the diffraction pattern in Fig. 2 shows significantly more variation than this, so two atoms per unit cell are insufficient to describe the full structure. The R factor is $R=0.44$. The Fourier sum used to calculate the Patterson function did not include integer-order reflections and hence only shows the layers with $c(2\times8)$ symmetry. One consequence is that the contour plot in Fig. 1(b) is distorted around bulk interatomic vectors and additional atoms with nearly 1×1 symmetry will not be clearly exposed in the plot.[19] Relaxed 1×1 structures with $c(2\times8)$ symmetry will show up as small peaks near bulk interatomic vectors with heights to first order proportional to the square of the displacement away from bulk lattice sites and positions shifted away from the interatomic vectors. This is what we see in Fig. 1(b). All remaining nonorigin peaks are weak and close to interatomic vectors from the bulk, and we must consider possible subsurface relaxations in order to complete the structure.

The structure factors measured with nearly zero momentum transfer in the direction normal to the surface yield information about the projection of the structure onto the surface plane. Hence, effectively only the first, second, and fourth layer from the bulk are visible as shown in Fig. 1(a). The adatoms are assumed to sit in symmetry sites on top of one of the layers. The subsurface atoms are relaxed according to the mirror lines coming from the $3m$ symmetry of the bulk and are connected in pairs as required by the forbidden quarter-order reflections. The independent atoms in the analysis are labeled in 1–8 in Fig. 1(a). The five atoms on the mirror lines are allowed to displace along the (2,1) direction whereas the three atoms off the mirror lines are allowed to displace in two directions: one radially towards the nearest adatom or rest atom and the other in the transverse direction. The adatoms and the atoms directly below them are fixed at (0,0) and (2,1). This gives, in total, eleven structural parameters and one scale factor to vary. The Debye-Waller B factor is kept fixed at the bulk value of 0.586 Å^2 for all atoms.[20] A least-squares analysis reduces the R factor to $R=0.21$. The uncertainties on the displacements are relatively large, on average estimated to be 0.08 Å. The displacements are therefore given in graphical form in Fig. 1(a). Due to the projection, the displacements shown are effective sums of displacements of the top atoms and the atoms directly below, and including more layers in the analysis cannot improve the agreement. However, the strain in the deeper layers is expected to be small and we will consider the displacements as arising from layer one, two, and four alone. The R factor is higher than expected from counting statistics and reproducibility between symmetry-equivalent reflections ($R=0.05$) and is due to the difficulty in obtaining correct integrated intensities as explained above.

IV. DISCUSSION

One of the significant features in Fig. 1(a) is the displacement pattern around the adatoms. Of the six atoms surrounding an adatom, three are pulled towards it while the other three are expelled. This is very similar to the pattern observed for Sn adatoms on the Ge(111) surface.[21–22] Here the Sn atoms are situated in T_4 sites, on top of second-layer Ge atoms and pull the three surrounding first-layer Ge atoms towards it, and also push the second-layer atom below it down which, via elastic strain, displaces the fourth-layer atoms away from the adatom (in projection). This suggests the assignment of the layers shown in Fig. 1(a) with the adatoms in T_4 sites, but measurements at a final momentum transfer in the direction normal to the surface are required for a final determination. Another important feature of Fig. 1(a) is the relaxation around the rest atom. This cannot be explained by elastic strain from the adatoms because that is expected to decay exponentially with distance. Instead it must be due to charge transfer from the dangling bonds on the adatoms to the dangling bonds on the rest atoms.[23] The charge transfer results in rehybridization and a displacement of the rest atom away from the surface,[24] thereby pulling in the surrounding atoms which in projection produces displacements towards the rest atom. The raising of the rest atom has also been observed in total-energy calculations on Si(111)-(7×7) (Ref. 25) and 2×2 adatom clusters.[26] One might speculate on the importance of the rest atoms. In the $c(2\times8)$ structure the the adatoms saturate 75% of the dangling bonds, whereas a 100% saturation can be obtained with the rest atom free $\sqrt{3}\times\sqrt{3}$ structure. Therefore, by taking part in the charge transfer the rest atom must play an important role in minimizing the total energy of the system.

The pairing of the atoms as assumed in the analysis does not hold in reality since it leads to frustration for the subsurface atoms labeled 2 and 3 in Fig. 1(a) and was only introduced to reduce the number of free parameters. Changing the assignments of the pairs does not alter the

displacement pattern significantly within the uncertainties. We have calculated the subsurface displacements by minimizing the elastic strain using a Keating model.[27] Although some deviation from the above-mentioned pairing was observed, the calculated intensities for the quarter-order reflections were always zero. Qualitative agreement with the displacements around the adatoms was obtained, but due to the charge transfer the Keating model fails to describe the rest atoms.

V. ANALYSIS OF THE DISORDER

We now turn to the disorder and the displacement of the eighth-order reflections. As seen in Fig. 3, only the eighth-order reflections are affected; the half-order reflections remain sharp. When the scan direction is orthogonal to the direction shown in Fig. 3, both eighth- and half-order peaks are sharp and unperturbed.

For a single domain this gives the alternating displacement pattern shown in Fig. 4(a). The peaks are displaced ± 0.005 in reciprocal lattice units, but measurements on other Ge(111) samples indicate that the absolute value depends on the preparation procedure of the surface. It shall be noted that neither the broadening and displacements of the peaks nor the tailing in Fig. 3 could be observed in the corresponding LEED pattern. However, during sample preparation the surfaces initially showed streaky $c(2\times 8)$ LEED patterns which became sharper after repeated sputtering-annealing cycles. The streaks were in the same directions as the broadening and tailing in Fig. 3 and must arise from the same kind of disorder.

Because only the eighth-order reflections are affected by the disorder, its origin must be found in different occupancies between sites which are all in-phase for half-order reflections. In the unit cell in Fig. 1(a) likely candidates are the sites at (2,1) and (2,2) which are related by inversion symmetry. Thus, if the next-nearest adatom interaction is sufficiently weak we would expect disorder in the occupancy of these two sites. The saturation of dangling bonds from three underlying substrate atoms by the adatom and the requirement of rest atoms means that there is a minimum distance between adatom, so shifting one adatom from site (2,1) to (2,2) implies shifting a full row of adatoms. This leaves only the two types of disorder shown in Fig. 4(a). Note that the $c(2\times 8)$ primitive cell consists of one 2×2 and one $c(4\times 2)$ unit cell and that the disorder can be described as faults in the long-range order of the $c(2\times 8)$ unit cells. The reciprocal lattices of the 2×2 and $c(4\times 2)$ structures are shown in Fig. 4(b). Since the eighth-order reflections are shifted towards the 2×2 lattice points we would intuitively expect the faults to be 2×2 unit cells.

We will now quantify the displacements of the eighth-order reflections by a simplified disorder model. A similar model has been derived for the missing row structure of Au(110)2×1.[28] A more general treatment is given by Lent and Cohen.[29] Consider the lines shown in Fig. 4(b) along the (2,1) direction and denote the rows of adatoms normal to this direction by index m. Let $P_m = 1$ if row m

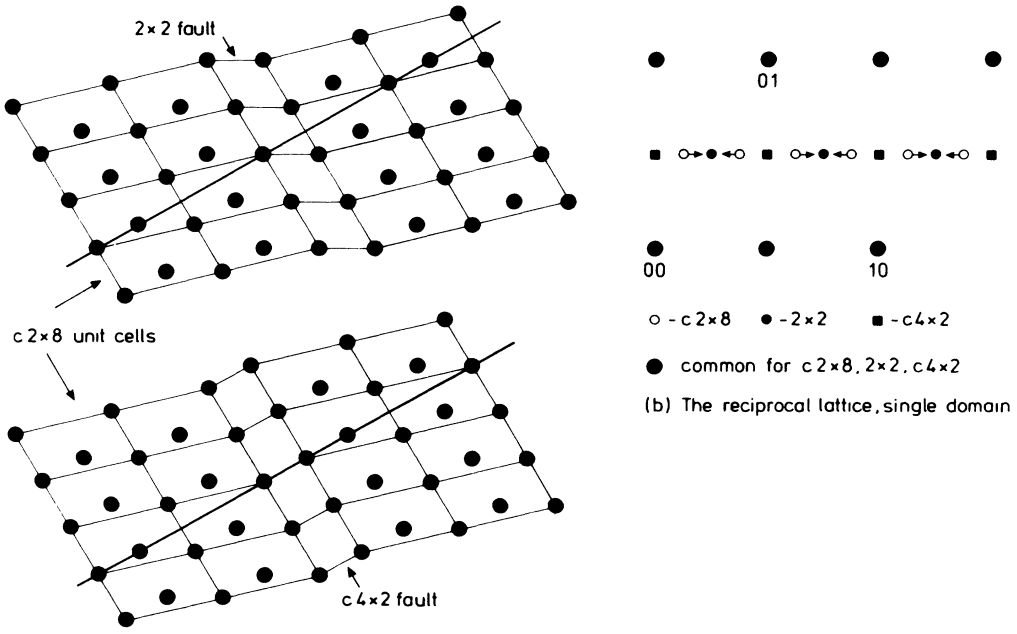

FIG. 4. (a) The two possible faults in the long-range order of $c(2\times 8)$ cells. The top shows rows of 2×2 cells as faults, the bottom shows rows of $c(4\times 2)$. The solid lines shown are used for indexing P_m, see the text. (b) The displacement pattern of the eighth-order reflections. Note that the reflections are displaced towards the 2×2 reciprocal-lattice positions, not the $c(4\times 2)$ positions.

has an adatom on the line and let $P_m=0$ if not. The sequence of P_m would then be 1100110011 for a regular $c(2\times8)$ structure. 2×2 faults give sequences like 110010011 (or equivalently 001101100) and $c(4\times2)$ faults 11001110011 (or 00110001100) sequences. We neglect for simplicity the subsurface relaxations and make the Fourier sum over the adatoms by first summing over each row in the (0,1) direction. Because there are no faults in that direction, this ensures that for a (h,k) reflection at least k remains unchanged. The sum in the (2,1) direction is then

$$G_{hk}=\sum_{m=0}^{\infty}[P_m+(1-P_m)e^{2\pi ik}]e^{2\pi im(2h+k)} . \tag{3}$$

For a half-order reflection k is an integer and the bracket in Eq. (3) is 1, so half-order reflections are unaffected. For eighth-order reflections the bracket is $2P_m-1$.

Let us assume that the faults are randomly distributed and described by a probability p for having a fault after a $c(2\times8)$ unit cell when going in the (2,1) direction. Let Q_m be the probability for $P_m=1$ given that $P_{m=0}=1$. It is simple to derive a recursive formula for Q_m, and we get

$$Q_m=\begin{cases}1-Q_{m-2}+p(Q_{m-2}-Q_{m-1}) & \text{for } 2\times2 \text{ faults}\\ 1-p-Q_{m-2}+p(Q_{m-1}+Q_{m-2}) & \text{for } c(4\times2) \text{ faults} .\end{cases} \tag{4}$$

Note that if $p=1$, Q_m follows the sequences 101010 or 11111 which corresponds to fault-free 2×2 or $c(4\times2)$ structures, respectively.

Because formula (4) is recursive, the summation in (3) is straightforward with P_m substituted by Q_m, and with the assumption that Q_m is symmetric we obtain

$$G_{hk}=\frac{1\pm ce^{2\pi i(2h+k)}}{1\pm pe^{2\pi i(2h+k)}+(1-p)e^{4\pi i(2h+k)}} ,$$

$$c=\frac{p(1-p)}{2-p} \tag{5}$$

where "+" corresponds to 2×2 faults and − corresponds to $c(4\times2)$ faults. Because Q_m is the pair correlation of P_m and because the sum in (3) has to be extended to include the terms $m=-\infty$ to $m=-1$, the intensity distribution is given by $I_{hk}\propto 2\ \mathrm{Re}(G_{hk})-1$. The solid curve in Fig. 3 shows the intensity distribution for 2×2 faults with $p=0.15$, the dashed curve has $p=0.4$. $c(4\times2)$ faults shift the peaks in the other direction. As seen, Eq. (5) can explain the displacement of the peaks but not fully the broadening or the tailing. This could be due to interaction between the faults giving larger areas with 2×2 cells, but could also arise from regions with different values for p within the surface area sampled in the diffraction experiment. The observation that only 2×2 unit cells occur as faults means that we can set up the inequality $E_{c(2\times8)}<E^{m}_{2\times2}<E_{c(2\times4)}$ for the total energies of the different unit cells, but since small clusters of both 2×2 and $c(4\times2)$ unit cells have been observed with STM,[14] all three energies must be nearly equal. The rows of 2×2 cells as faults in the $c(2\times8)$ structure has also recently been observed in STM images, where it was shown that they originate at one boundary between two 120° orientationally related $c(2\times8)$ domains and extend all the way through the $c(2\times8)$ domain to the next boundary.[30] The disorder is different from that observed by LEED at higher temperatures where a model with hexagonal domains of 2×2 cells and walls of $c(4\times2)$ cells was proposed.[17]

VI. SUMMARY

In summary, with surface x-ray diffraction we have confirmed the simple adatom model recently proposed for Ge(111)-$c(2\times8)$ and shown that the long-range order of the $c(2\times8)$ structure is disturbed by extra rows of 2×2 unit cells.

ACKNOWLEDGMENTS

We wish to thank the staff of HASYLAB for their hospitality and assistance and R. S. Becker, J. A. Golovchenko, K. Kjær, D. Vanderbilt, and H. Zabel for fruitful and stimulating discussions. The work was supported by the Danish Natural Science Foundation and the German Federal Minister for Science and Technology under Project No. 05-390-CAB.

*Present address: Risø Natinal Laboratory, DK-4000 Roskilde, Denmark.

[1]K. Shoji, M. Hyodo, H. Ueba, and C. Tatsuyama, Jpn. J. Appl. Phys. **22**, L200 (1983).

[2]H. J. Gossmann, J. C. Bean, L. C. Feldman, and W. M. Gibson, Surf. Sci. **138**, L175 (1984).

[3]E. G. McRae and R. A. Malic, Surf. Sci. **165**, 191 (1986).

[4]I. Ichikawa and S. Ino, Surf. Sci. **105**, 395 (1981).

[5]R. E. Schlier and H. E. Farnsworth, J. Chem. Phys. **30**, 917 (1959).

[6]H. J. Gossman, J. C. Bean, L. C. Feldman, E. G. McRae, and I. K. Robinson, Phys. Rev. Lett. **55**, 1106 (1985).

[7]K. Takayanagi, Y. Tanishiro, S. Takahashi, and M. Takahashi, Surf. Sci. **164**, 367 (1985).

[8]K. Takayanagi and Y. Tanishiro, Phys. Rev. B **34**, 1034 (1986); K. Takayanagi, Y. Tanishiro, and K. Kajiyama, J. Vac. Sci. Technol. B **4**, 1074 (1986).

[9]D. Vanderbilt, Phys. Rev. B **36**, 6209 (1987).

[10]J. J. Lander, G. W. Gobeli, and J. Morrison, J. Appl. Phys. **34**, 2298 (1963).

[11]D. J. Chadi and C. Chiang, Phys. Rev. B **23**, 1843 (1981).
[12]W. S. Yang and F. Jona, Phys. Rev. B **29**, 899 (1984).
[13]We will label the structure $c(2\times8)$ as usual in the literature, however strictly speaking we mean $c(8\times2)$.
[14]R. S. Becker, J. A. Golovchenko, and B. S. Swartzentruber, Phys. Rev. Lett. **54**, 2678 (1985).
[15]P. M. J. Marée, K. Nakagawa, J. F. van der Veen, and R. M. Tromp, Phys. Rev. B **38**, 1585 (1988).
[16]R. J. Culbertson, Y. Kuk, and L. C. Feldman, Surf. Sci. **167**, 127 (1986).
[17]R. J. Phaneuf and M. B. Webb, Surf. Sci. **164**, 167 (1985).
[18]B. E. Warren, *X-Ray Diffraction* (Addison-Wesley, Reading, Mass., 1968).
[19]J. Bohr, R. Feidenhans'l, M. Nielsen, M. Toney, R. L. Johnson, and I. K. Robinson, Phys. Rev. Lett. **56**, 2878 (1986).
[20]B. W. Batterman and D. R. Chipman, Phys. Rev. **127**, 690 (1962).
[21]J. S. Pedersen, R. Feidenhans'l, M. Nielsen, K. Kjær, F. Grey, and R. L. Johnson, Surf. Sci. **189/190**, 1047 (1987).
[22]J. S. Pedersen, Ph.D. thesis, Copenhagen University (1988). Available as Report No. Risø-M-2713 on request to the Risø Library.
[23]J. E. Northrup, Phys. Rev. Lett. **57**, 154 (1986).
[24]M. Schlüter, J. R. Chelikowsky, S. G. Louie, and M. L. Cohen, Phys. Rev. B **12**, 4200 (1975).
[25]G.-X. Qian and D. J. Chadi, Phys. Rev. B **35**, 1288 (1987).
[26]D. Vanderbilt (private communication).
[27]P. N. Keating, Phys. Rev. **145**, 637 (1966).
[28]I.K. Robinson, *The Structure of Surfaces I,* edited by M. A. Van Hove and S. Y. Tong (Springer-Verlag, Berlin, 1985), p. 60.
[29]C. S. Lent and P. I. Cohen, Surf. Sci. **139**, 121 (1984).
[30]R. S. Becker and J. A. Golovchenko (private communication).